Fiddling the Twiddle Constants - Fault Injection Analysis of the Number Theoretic Transform

Prasanna Ravi[1,2], Bolin Yang[3], Shivam Bhasin[1], Fan Zhang[4] and Anupam Chattopadhyay[1,2]

[1] Temasek Laboratories, Nanyang Technological University, Singapore
[2] School of Computer Science and Engineering, Nanyang Technological University, Singapore
[3] College of Information Science and Electronic Engineering, Zhejiang University, China
[4] Zhejiang University, China

prasanna.ravi@ntu.edu.sg yangbolin@zju.edu.cn sbhasin@ntu.edu.sg
anupam@ntu.edu.sg fanzhang@zju.edu.cn

Abstract.
In this work, we present the first fault injection analysis of the Number Theoretic Transform (NTT). The NTT is an integral computation unit, widely used for polynomial multiplication in several structured lattice-based key encapsulation mechanisms (KEMs) and digital signature schemes. We identify a critical single fault vulnerability in the NTT, which severely reduces the entropy of its output. This in turn enables us to perform a wide-range of attacks applicable to lattice-based KEMs as well as signature schemes. In particular, we demonstrate novel key recovery and message recovery attacks targeting the key generation and encryption procedure of Kyber KEM. We also propose novel existential forgery attacks targeting deterministic and probabilistic signing procedure of Dilithium, followed by a novel verification bypass attack targeting its verification procedure. All proposed exploits are demonstrated with high success rate using electromagnetic fault injection on optimized implementations of Kyber and Dilithium, from the open-source *pqm4* library on the ARM Cortex-M4 microcontroller.

Keywords: No keywords given.

1 Introduction

The NIST standardization process for *post-quantum cryptography* is in its third and final round, at the time of writing of this paper, with the first draft standards expected to be released in 2023. While implementation performance and theoretical security guarantees served as the main criteria in the initial rounds, resistance against *side-channel attacks* (SCA) and *fault injection attacks* (FIA) emerged as an important criterion in the final round, as also clearly stated by NIST at several instances [AH21,RR21]. More importantly, it could serve as a *key distinguisher* for the final selection of candidates, especially amongst those schemes with tightly matched security and efficiency.

Amongst the seven main finalists for *key encapsulation mechanisms* (KEMs) and *digital signatures*, five schemes base their security on hard problems over structured lattices [AASA+20]. These schemes are particularly attractive for constrained embedded devices, owing to their relatively small public key sizes and highly competitive runtimes. They typically operate over polynomials in polynomial rings, and notably, *polynomial multiplication* is one of the most computationally intensive operations in practical implementations of these schemes. Among the several known techniques for polynomial multiplication such as the schoolbook multiplier, Toom-Cook [Too63] and Karatsuba [Kar63], the Number

Theoretic Transform (NTT) based polynomial multiplication [CT65] is one of the most widely adopted techniques, owing to its superior run-time complexity and a compact design. Over the years, there has been a sustained effort by the cryptographic community to improve the performance of NTT for lattice-based schemes on a wide-range of hardware and software platforms [RVM+14, POG15, BKS19, ACC+22, CHK+21]. As a result, the use of NTT for polynomial multiplication yields the fastest implementation for several finalist candidates such as Kyber [ABD+20], Dilithium [LDK+17], Saber [DKSRV20] and NTRU [CDH+19].

While NTT provides significant implementation benefits, it also manipulates sensitive variables, thereby serving as an attractive target for SCA and FIA. While the side-channel resistance of NTT has been studied by a number of works [PPM17, PP19, RPBC20], its susceptibility to fault injection attacks has not recieved much attention. Given its widespread use in lattice-based schemes, this raises a critical question whether *the NTT or more importantly its implementations contain hidden vulnerabilities that can be exploited through FIA to compromise the security of lattice-based schemes.*

Our Contribution: In this work, we answer this question positively, by presenting the first *fault injection analysis* of the NTT. Our work relies on a key observation that *zeroization of the twiddle contants* significantly reduces the entropy in the NTT output, which inturn severely impacts the security of lattice-based schemes. To analyze the feasibility of such a fault, we perform a detailed study of the optimized implementations of NTT used in Kyber (representative of KEMs) and Dilithium (representative of signature schemes) on the ARM Cortex-M4 microcontroller using electromagnetic fault injection. We identified a critical fault vulnerability in their implementations, which enables zeroization of all the twiddle constants using a *single targeted fault.* This enables practical key/message recovery attacks on Kyber KEM and forgery attacks on Dilithium. To the best of our knowledge, we present first practical forgery attack on probabilistic variant[1] and *verification bypass* attack on the verification procedure of Dilithium.

Organization of the Paper

In Section 2, we provide a generic description of Kyber and Dilithium, and provide some background about NTT as well as related prior work. In Section 3, we describe the identified vulnerability in the NTT, and a detailed analysis of the same over practical implementations of NTT in Kyber and Dilithium. In Sections 4 and 5, we demonstrate exploitation of the identified vulnerability in Kyber and Dilithium respectively. In Section 6, we perform experimental validation of our attacks using EMFI, followed by conclusion and mitigation in Section 7.

2 Background

2.1 Notation

Let q be a prime number, and the field of integers modulo q be denoted as $\mathbb{Z}_q$. Schemes such as Kyber and Dilithium operate over polynomials in polynomial rings. The polynomial ring $\mathbb{Z}_q[x]/\phi(x)$ is denoted as R_q where $\phi(x) = x^n + 1$ is a cyclotomic polynomial with n being a power of 2. Polynomials in R_q are denoted using regular font letters (i.e.) $a \in R_q$. The i^{th} coefficient of $a \in R_q$ is denoted as $a_i \in \mathbb{Z}_q$. For $a \in R_q$, $\ell_\infty(a)$ denotes the largest absolute value of a coefficient of a in $\mathbb{Z}_q$. A vector of polynomials in R_q is denoted using bold lower case letters (i.e.) $\mathbf{a} \in R_q^k$ with $k > 1$, and a matrix of polynomials in R_q

[1] Islam et al. [IMS+22] recently proposed a rowhammer based attack on deterministic and probabilistic Dilithium but its final complexity still remains as 2^{89}, while we report a full break.

is denoted using bold upper case letters (i.e.) $\mathbf{A} \in R_q^{k\times\ell}$ with $(k,\ell) > 1$. The element $\mathbf{A}[i][j]$ denotes the polynomial in row i and j of $\mathbf{A} \in R_q^{k\times\ell}$. Transpose of a matrix $\mathbf{A}$ is denoted as $\mathbf{A}^T$. Multiplication of polynomials $(a,b) \in R_q$ is denoted as $c = a \cdot b \in R_q$. Pointwise/Coefficient-wise multiplication of two polynomials $(a,b) \in R_q$ is denoted as $c = a \circ b \in R_q$. We denote $\mathcal{B}$ as a byte array, where the i^{th} byte is denoted as $\mathcal{B}[i]$. For a given element a ($\mathbb{Z}_q$ or R_q or $R_q^{k\times\ell}$), its corresponding faulty value is denoted as a^* and we utilize this notation for description of our attacks. The NTT representation of a polynomial $a \in R_q$ is denoted as $\hat{a} \in R_q$, and the same notation also applies to modules of higher dimension.

2.2 Kyber

Kyber is a Chosen-Ciphertext Attack (CCA) secure KEM based on the Module Learning With Errors (M-LWE) problem. Computations are done over modules in dimension $(k \times k)$ (i.e) $R_q^{k\times k}$ where $R_q = \mathbb{Z}_q[x]/(x^n+1)$, $q = 3329$ and $n = 256$. Kyber comes in three security levels, Kyber512 (NIST Level 1), Kyber-768 (Level 3) and Kyber-1024 (Level 5) with $k = 2, 3$ and 4 respectively. The parameters q, n and the modular polynomial $\phi(x) = x^n + 1$ are chosen, so as to allow the use of the Number Theoretic Transform (NTT) for polynomial multiplication in R_q.

The CCA-secure Kyber KEM contains in its core, a Chosen-Plaintext Attack (CPA) secure PKE. Refer to Algorithm 1 for a simplified description of the key-generation and encryption procedures of CPA secure PKE of Kyber. We do not describe the decryption procedure, as it is not a target of our attacks. The function Sample_U samples from a uniform distribution, Sample_B samples from a binomial distribution; Expand expands a small seed into a uniformly random matrix in $R_q^{k\times k}$. The function $\mathsf{Compress}(u,d)$ lossily compresses $u \in \mathbb{Z}_q$ into $v \in \mathbb{Z}_{2^d}$ with $q > 2^d$, while $\mathsf{Decompress}(v,d)$ extrapolates $v \in \mathbb{Z}_{2^d}$ into $u' \in \mathbb{Z}_q$. The CPA secure PKE is converted into a CCA secure KEM using the Fujisaki-Okamoto transformation [FO99]. The transformation enables to check for the validity of the received ciphertext upon decryption, by performing a *re-encryption* of the decrypted message. This enables to detect invalid ciphertexts, thereby offering concrete theoretical security guarantees against chosen-ciphertext attacks. We refer the reader to [ABD+20] for more details on CCA secure Kyber KEM.

2.3 Dilithium

Dilithium is a lattice-based signature scheme secure, whose security is based on the Module LWE (M-LWE) and Module SIS (M-SIS) problem. Dilithium operates over the module $R_q^{k\times\ell}$ with $(k,\ell) > 1$ where $R_q = \mathbb{Z}[x]/(x^n+1)$, $n = 256$ and $q = 2^{23} - 2^{17} - 1$. This choice of parameters allows the use of NTT for polynomial multiplication in R_q. Dilithium also comes in three security levels: Dilithium2 with $(k,\ell) = (4,4)$ at NIST Level 2, Dilithium3 with $(k,\ell) = (6,5)$ at NIST Level 3 and Dilithium5 with $(k,\ell) = (8,7)$ at NIST Level 5. There are two variants of Dilithium: (1) Deterministic (2) Probabilistic/Randomized, which only subtly differ in the way randomness is used in the signing procedure. The signing procedure of the deterministic Dilithium does not utilize external randomness and can generate only a single signature for a given message. The randomized variant however utilizes external randomness and thus generates a different signature, for a given message in each execution.

Refer Alg.2 for the key generation, signing and verification procedures of Dilithium. The functions Sample_U, Sample_B and Expand perform the same functions as in Kyber, albeit with different parameters. Dilithium also uses a number of rounding functions such as Power2Round, HighBits, LowBits, MakeHint and UseHint, whose details can be found in [LDK+17]. The key generation procedure simply involves generation of an LWE instance $\mathbf{t}$ (Line 4). Subsequently, the LWE instance is split into higher and lower order bits $\mathbf{t_1}$

Algorithm 1 CPA Secure Kyber PKE (Simplified)

procedure CPA.KeyGen
  $seed_A \in \mathcal{B} \leftarrow \mathsf{Sample}_U()$ ▷ Generate uniform $Seed_A$
  $seed_B \in \mathcal{B} \leftarrow \mathsf{Sample}_U()$ ▷ Generate uniform $Seed_B$
  $\hat{\mathbf{A}} = \mathsf{NTT}(\mathbf{A}) \in R_q^{k \times k} \leftarrow \mathsf{Expand}(seed_A)$ ▷ Expand $seed_A$ into $\hat{\mathbf{A}}$ in NTT domain
  $\mathbf{s} \in R_q^k \leftarrow \mathsf{Sample}_B(seed_B, coins_s)$ ▷ Sample secret $\mathbf{s}$ using $(Seed_B, coins_s)$
  $\mathbf{e} \in R_q^k \leftarrow \mathsf{Sample}_B(seed_B, coins_e)$ ▷ Sample error $\mathbf{e}$ using $(Seed_B, coins_e)$
  $\hat{\mathbf{s}} \in R_q^k \leftarrow \mathsf{NTT}(\mathbf{s})$ ▷ $\mathsf{NTT}(\mathbf{s})$
  $\hat{\mathbf{e}} \in R_q^k \leftarrow \mathsf{NTT}(\mathbf{e})$ ▷ $\mathsf{NTT}(\mathbf{e})$
  $\hat{\mathbf{t}} = \hat{\mathbf{A}} \circ \hat{\mathbf{s}} + \hat{\mathbf{e}}$ ▷ $\mathbf{t} = \mathbf{A} \cdot \mathbf{s} + \mathbf{e}$ in NTT domain
  Return $(pk = (seed_A, \hat{\mathbf{t}}), sk = (\hat{\mathbf{s}}))$
end procedure

procedure CPA.Encrypt$(pk, m \in \{0,1\}^{256}, seed_R \in \{0,1\}^{256})$
  $\hat{\mathbf{A}} \in R_q^{k \times k} \leftarrow \mathsf{Expand}(seed_A)$
  $\mathbf{r} \in R_q^k \leftarrow \mathsf{Sample}_B(seed_R, coins_0)$ ▷ Sample $\mathbf{r}$ using $(Seed_R, coins_0)$
  $\mathbf{e_1} \in R_q^k \leftarrow \mathsf{Sample}_B(seed_R, coins_1)$ ▷ Sample $\mathbf{e}_1$ using $(Seed_R, coins_1)$
  $\mathbf{e_2} \in R_q^k \leftarrow \mathsf{Sample}_B(seed_R, coins_2)$ ▷ Sample $\mathbf{e}_2$ using $(Seed_R, coins_2)$
  $\hat{\mathbf{r}} \in R_q^k \leftarrow \mathsf{NTT}(\mathbf{r})$ ▷ $\mathsf{NTT}(\mathbf{r})$
  $\mathbf{u} \in R_q^k \leftarrow \mathsf{INTT}(\mathbf{A}^T \circ \hat{\mathbf{r}}) + \mathbf{e_1}$ ▷ $\mathbf{u} = \mathbf{A}^T \cdot \mathbf{r} + \mathbf{e_1}$
  $v \in R_q \leftarrow \mathsf{INTT}(\hat{t}^T \circ \hat{\mathbf{r}}) + \mathbf{e_2} + \mathsf{Decompress}(m, 1)$ ▷ $\mathbf{v} = \mathbf{t}^T \cdot \mathbf{r} + \mathbf{e_2} + \mathsf{Encode}(m)$
  Return $ct = \mathsf{Compress}(\mathbf{u}, d_1), \mathsf{Compress}(v, d_2)$
end procedure

and $\mathbf{t_0}$ respectively (Line 5), where $\mathbf{t_1}$ forms part of the public key, while $\mathbf{t_0}$ becomes part of the secret key.

The signing procedure of Dilithium is based on the "Fiat-Shamir with Aborts" framework where the signature is repeatedly generated and rejected until it satisfies a given set of conditions [Lyu09]. The message m is first hashed with a public value tr to generate μ (Line 11). The abort loop (Line 18-31) starts by generating an ephemeral nonce $\mathbf{y} \in R_q^\ell$, using a seed ρ. For the deterministic variant, the seed ρ is obtained by hashing μ with a secret nonce K (Line 14), while the probabilistic variant randomly samples the seed ρ from a uniform distribution (Line 16). This is the only differentiator between the two variants. The nonce $\mathbf{y}$ along with the public key component $\mathbf{A}$ is then used to calculate a sparse challenge polynomial $c \in R_q$ (Line 22), whose 60 coefficients are either ± 1, while the other 196 coefficients are 0. Subsequently, the challenge c, nonce $\mathbf{y}$ and secret $\mathbf{s}_1$, are used to compute the primary signature component $\mathbf{z}$ (Line 24). Then, a hint vector $\mathbf{h}$ is generated and output as part of the signature σ. The abort loop contains several conditional checks (Line 27), which should be simultaneously satisfied to terminate the abort loop and generate the signature $\sigma = (\mathbf{z}, \mathbf{h}, c)$.

The verification procedure utilizes the signature σ and the public key pk to recompute the challenge polynomial $\bar{c}$ (Line 38), which is then compared with the received challenge c, along with other checks (Line 39). If all the checks are satisified, then the verification is successful, else it is a failure.

2.4 Number Theoretic Transform

The Number Theoretic Transform (NTT) is utilized as a building block for polynomial multiplication operation in several structured lattice-based schemes. While schemes such as Kyber and Dilithium were designed with *NTT-friendly* parameters to allow use of NTT, other schemes such as Saber, NTRU and NTRU Prime were designed with *NTT-*

Algorithm 2 Dilithium Signature scheme (Simplified)

procedure KeyGen
  $(seed_A, seed_S, K) \in \mathcal{B} \leftarrow \mathsf{Sample}_U()$; $\mathbf{s_1}, \mathbf{s_2} \in (R_q^\ell \times R_q^k) \leftarrow \mathsf{Sample}_B(seed_S)$
  $\mathbf{A} \in R_q^{k\times\ell} \leftarrow \mathsf{Expand}(seed_A)$
  $\mathbf{t} = \mathbf{A} \cdot \mathbf{s_1} + \mathbf{s_2}$ ▷ Generate LWE instance $\mathbf{t}$
  $(\mathbf{t_1}, \mathbf{t_0}) \leftarrow \mathsf{Power2Round}(\mathbf{t})$ ▷ Split $\mathbf{t}$ as $\mathbf{t_1} \cdot 2^d + \mathbf{t_0}$
  $tr \in \mathcal{B} \leftarrow \mathcal{H}(seed_A \| \mathbf{t}_1)$
  $pk = (seed_A, \mathbf{t_1}), sk = (seed_A, K, tr, \mathbf{s_1}, \mathbf{s_2}, \mathbf{t_0})$
end procedure

---

procedure Sign(sk, M)
  $\hat{\mathbf{A}} \in R_q^{k\times\ell} \leftarrow \mathsf{Expand}(seed_A)$
  $\mu \in \{0,1\}^{512} \leftarrow \mathcal{H}(tr \| M)$ ▷ Hash m with public value tr
  $\kappa \leftarrow 0$; $(\mathbf{z}, \mathbf{h}) \leftarrow \perp$
  if Deterministic **then**
    $\rho \in R_q^\ell \leftarrow \mathcal{H}(K \| \mu)$ ▷ Generate seed ρ using message and secret seed K
  else
    $\rho \in R_q^\ell \leftarrow \mathsf{Sample}_U()$ ▷ Generate uniform seed ρ
  end if
  while $(\mathbf{z}, \mathbf{h}) = \perp$ **do** ▷ Start of Abort Loop
    $\mathbf{y} \leftarrow \mathsf{Sample}_Y(\rho \| \kappa)$
    $\hat{\mathbf{y}} = \mathsf{NTT}(\mathbf{y})$ ▷ $\mathsf{NTT}(y)$
    $\mathbf{w} \leftarrow \mathsf{INTT}(\hat{\mathbf{A}} \circ \hat{\mathbf{y}})$; $\mathbf{w_1} \leftarrow \mathsf{HighBits}(\mathbf{w})$ ▷ $\mathsf{w_1} = \mathsf{HighBits}(\mathbf{A} \cdot \mathbf{y})$
    $c \in R_q \leftarrow \mathcal{H}(\mu \| \mathbf{w_1})$ ▷ Generate Sparse Challenge c
    $\hat{c} = \mathsf{NTT}(c)$ ▷ $\mathsf{NTT}(c)$
    $\mathbf{z} = \mathsf{INTT}(\hat{\mathbf{c}} \circ \hat{\mathbf{s}}_\mathbf{1}) + \mathbf{y}$ ▷ $\mathbf{z} = \mathbf{s_1} \cdot c + \mathbf{y}$
    ...
    Compute Hint Vector $\mathbf{h}$
    if Conditional Checks Not Satisfied **then**
      $(\mathbf{z}, \mathbf{h}) = \perp$
      $\kappa = \kappa + 1$
    end if
  end while
  $\sigma = (\mathbf{z}, \mathbf{h}, c)$
end procedure

---

procedure Verify$(pk, M, \sigma = (\mathbf{z}, \mathbf{h}, c))$
  $\mu \in \{0,1\}^{512} \leftarrow \mathcal{H}(tr \| M)$
  $\hat{c} = \mathsf{NTT}(c)$ ▷ $\mathsf{NTT}(c)$
  $\mathbf{w}_1' := \mathsf{UseHint}(\mathbf{h}, \mathbf{A} \cdot \mathbf{z} - \mathsf{INTT}(\hat{c} \circ \hat{\mathbf{t}}_\mathbf{1} \cdot 2^d, 2\gamma_2)$
  $\bar{c} = \mathcal{H}(\mu, \mathbf{w}_1')$
  if $(\bar{c} == c)$ and (norm of $\mathbf{z}$ and $\mathbf{h}$ are valid) **then**
    Return Pass
  else
    Return Fail
  end if
end procedure

unfriendly parameters, thereby relying on other techniques such as Toom-Cook [Coo66] and Karatsuba [Kar63] for polynomial multiplication. However, recent works such as [ACC+21, CHK+21, ACC+22] have shown that NTT can be indeed be used in these schemes, which also leads to significant improvement in performance over non-NTT based approaches.

The NTT is simply a bijective mapping for a polynomial $p \in R_q$ from a *normal* domain into an alternative represetation $\hat{p} \in R_q$ in the *NTT domain* as follows:

$$\hat{p}_j = \sum_{i=0}^{n-1} p_i \cdot \omega^{i \cdot j} \tag{1}$$

where $j \in [0, n-1]$ and ω is the n^{th} root of unity in the operating ring $\mathbb{Z}_q$. The corresponding inverse operation named Inverse NTT (denoted as INTT) maps $\hat{p}$ in the NTT domain back to p in the normal domain. The use of NTT requires either the n^{th} root of unity (ω) or $2n^{\text{th}}$ root of unity (ψ) in the underlying ring $\mathbb{Z}_q$ ($\psi^2 = \omega$), which can be ensured through appropriate choices for the parameters (n, q). The powers of ω and ψ that are used within the NTT computation are commonly referred to as *twiddle constants*. NTT based multiplication of two polynomials $\mathbf{a}$ and $\mathbf{b}$ in R_q is typically done as follows:

$$\mathbf{c} = \text{INTT}(\text{NTT}(\mathbf{a}) \circ \text{NTT}(\mathbf{b})). \tag{2}$$

The NTT over an n point sequence is performed using the well-known *butterfly* network, which operates over several layers/stages. The atomic operation within the NTT computation is denoted as the *butterfly* operation. A butterfly operation takes as inputs $(a, b) \in \mathbb{Z}_q^2$ and a twiddle constant w, and produces outputs $(c, d) \in \mathbb{Z}_q^2$. There are two types of butterfly operations, which can be interchangeably used in the NTT/INTT: (1) Cooley-Tukey (CT) butterfly [CT65] in Eqn.3 and (2) Gentleman-Sande (GS) butterfly [GS66] in Eqn.4. An NTT/INTT of size $n = 2^k$ typically consists of k stages with each stage containing $n/2$ butterfly operations. Refer Fig.1 for the data-flow graph of a CT-butterfly based NTT for an input sequence with length $n = 8$.

$$\begin{aligned} c &= a + b \cdot w \\ d &= a - b \cdot w, \end{aligned} \tag{3}$$

$$\begin{aligned} c &= a + b \\ d &= (a - b) \cdot w, \end{aligned} \tag{4}$$

The underlying integer ring $\mathbb{Z}_q$ of Dilithium contains both ω and ψ, ensuring complete factorization of $(x^n + 1)$ into linear factors (degree 1). This enables to use a *complete* NTT with $k = log_2(n)$ stages. However, the ring $\mathbb{Z}_q$ of Kyber only contains ω, which implies that $(x^n + 1)$ can only be factored into $n/2$ quadratic factors (degree 2). Thus, the last stage of NTT/INTT in Kyber is skipped and the NTT output contains $n/2$ elements. Thus, Kyber relies on the use of an *incomplete* NTT with $k - 1$ stages.

2.5 Prior Works

This subsection highlights notable works exploring vulnerability of lattice-based schemes against fault-injection attacks.

2.5.1 Fault Attacks on Signature Schemes

Bindel *et al.* [BBK] reported the first fault analysis of lattice-based signatures, proposing several fault attacks on signature schemes such as GLP [GLP12] and BLISS [DDLL13]. Their attacks target several operations across the key generation, signing and verification procedures, assuming various fault models such as randomization faults, zeroization faults and skipping faults. However, their attacks either rely on difficult-to-achieve fault models, or require impractically high number of faults. Further, Espitau *et al.* [EFGT16] proposed a novel *loop abort* fault attack on the signing procedure of BLISS, relying on only a single fault to prematurely abort the generation of the nonce $\mathbf{y}$ (equivalent to Line 19 in Alg.2), leading to key recovery with only a single fault. However, their attack assumes that

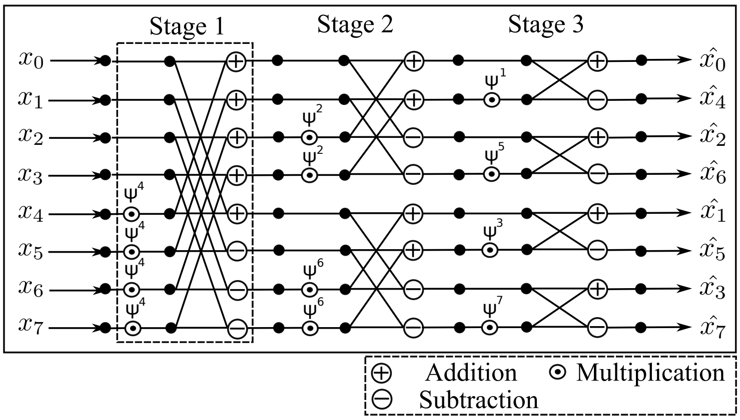

Figure 1: Data flow graphs of CT-butterfly based NTT for size $n = 8$.

the nonce is initialized with a 0 value, which always might not hold true, as shown in [RJH+19].

Bruinderink and Pessl [BP18] presented a novel and powerful differential fault attack on deterministic Dilithium and qTESLA. Their attack could recover the secret key with only a single random fault, injected anywhere within 68% of the execution time of the signing procedure. Subsequently, Ravi *et al.* proposed *skip-addition* fault attacks on deterministic Dilithium, targeting the final addition operation to generate the signature component $\mathbf{z}$ (Line 24 in Alg.2). Their attack however requires a few hundred faulty signatures to recover the secret key. More recently, Islam *et al.* [IMS+22] proposed a signature correction attack, applicable to both the deterministic and probabilistic variants of Dilithium. It works by injecting bit flips on the secret key stored in memory, and subsequently utilizing a correction algorithm to recover the value of the flipped secret bits, one at a time. While they utilize Rowhammer as an attack vector on the AVX2 optimized implementation of Dilithium, the feasibility of injecting precise bit flips in memory, on constrained embedded targets such as ours (ARM Cortex-M4) is not clear, and atleast non-trivial at best.

2.5.2 Fault Attacks on KEMs

Ravi *et al.* [RRB+19] proposed the first practical fault attack on lattice-based KEMs such as Kyber, NewHope and Frodo. Their attack forces nonce reuse through EMFI, resulting in generation of weak LWE instances in the key generation and encryption procedure, that leads to trivial key recovery and message recovery attacks. Other reported fault attacks on lattice-based KEMs mainly target the decapsulation procedure, to recover the long-term secret key. Pessl and Prokop proposed a novel fault-assisted chosen-ciphertext attack [PP21] on Kyber KEM. Their attack works by injecting targeted faults in the message decoding procedure, and subsequently utilizing information about the success/failure of decapsulation, as a decryption failure oracle. This results in key recovery in a few thousand chosen-ciphertexts. While this attack can be thwarted by shuffling the message decoding operation, Hermelink *et al.* [HPP21] proposed an improved attack that can defeat the shuffling protection, but relies on a slightly stronger fault model of injecting targeted bit flip faults in memory.

Delvaux and Pozo [DDP21] further improved the attack of Hermelink *et al.* by expanding the attack surface to several operations within the decapsulation procedure, while also working with a variety of more relaxed fault models. Xagawa *et al.* [XIU+21] recently demonstrated that the obvious target of the final equality check in the decapsulation procedure can be easily skipped in several lattice-based KEMs, thereby downgrading from

CCA security to CPA security for key recovery through chosen-ciphertext attacks.

2.5.3 Motivation

The reported fault attacks on KEMs and signature schemes have predominantly been orthogonal in nature, with most attacks being specific either to KEMs or signature schemes. In this respect, we identify the Number Theoretic Transform (NTT) as a commonality, as it is used in both KEMs and signature schemes. While the side-channel resistance of NTT has been studied by a number of works [PPM17, PP19, RPBC20], there are no known fault attacks that exploit the inherent nature of the NTT. Given its widespread usage in several schemes, it becomes imperative to analyze its susceptibility to FIA and identify suitable countermeasures for protection. Thus, we perform the first fault injection analysis of the NTT, and identify a critical vulnerability in practical implementations of NTT, which can be exploited to mount a wide variety of attacks on lattice-based KEMs as well as signature schemes.

3 Fault Vulnerability of NTT

3.1 Intuition

We start by analyzing a single CT butterfly operation (described in Eqn.3), commonly used to implement the forward NTT. Its inputs are $(x_0, x_1) \in \mathbb{Z}_q$, twiddle constant w, and outputs are $(y_0, y_1) = ((x_0 + x_1 \cdot w), (x_0 - x_0 \cdot w))$. We consider the possibility of injecting faults to zeroize the twiddle factor w. As a result, the faulty outputs of the butterfly are $(y_0^*, y_1^*) = (x_0, x_0)$, with no effect of x_1 on the faulty output. We now extend the same fault to all the butterflies in a single stage of NTT (Refer to Stage-1 of NTT in Fig.1). Let the input to the stage be x_i for $i \in [0, n-1]$ and its output be y_i for $i \in [0, n-1]$. If all of its twiddle constants are 0, then the output is given as:

$$y_i = \begin{cases} x_i, & \text{for } i < n/2 \\ x_{i-(n/2)}, & \text{otherwise} \end{cases} \tag{5}$$

We observe that the entropy of the output is reduced by half. If we extend the same fault to the entire NTT, then the final output of NTT $\hat{x}$ is simply $\hat{x}_i = x_0 \; \forall \, i \in [0, n-1]$. In essence, the entropy of the output is reduced by half for every stage, with the final output only containing a single element x_0 repeated n times. Thus, zeroizing the twiddle constants produces a faulty output with very low entropy. If this faulty NTT output is utilized for polynomial multiplication with $z \in R_q$ (i.e.) $x \cdot z \in R_q$, then the faulty product is $x^* \cdot z \in R_q$ where x^* is given as,

$$x_i^* = \begin{cases} x_0, & \text{if } i = 0 \\ 0, & \text{otherwise} \end{cases} \tag{6}$$

Thus, faulting the NTT of x in this manner has the effect of *implicitly changing* x to x^* with low entropy, with only a single non-zero coefficient. While this applies for schemes such as Dilithium which utilize a complete NTT, Kyber utilizes an incomplete NTT with last stage skipped. The implicitly modified faulty input x^* in case of Kyber KEM is given as:

$$x_i^* = \begin{cases} x_i, & \text{for } i = \{0, 1\} \\ 0, & \text{otherwise} \end{cases} \tag{7}$$

with two non-zero coefficients. Thus, the entropy of the faulty input x^* depends upon the number of stages in the NTT. *While zeroization of all the twiddle constants comes* *across as a strong assumption, we have identified a critical fault vulnerability in practical implementations of NTT in several schemes, which enables zeroization of twiddle constants with only a single targeted fault.*

3.2 Analysing Practical NTT Implementations

Algorithm 3 Assembly Optimized NTT of Kyber in *pqm4* library [KRSS19] (Simplified)

```
ldr r1, [pc, #4]                 ▷ Loading twiddle-ptr from address (pc+4) to register r1

            ***Start of NTT Assembly Routine***

n ← 16
while n > 0 do                                   ▷ First stage (Stage 1,2,3)
    load poly
    ldrh twiddle, [twiddle-ptr]                  ▷ Loading twiddle from twiddle-ptr
    doublebutterfly (poly, twiddle)
    ldr twiddle, [twiddle-ptr, #2]               ▷ Loading twiddle from (twiddle-ptr+2)
    doublebutterfly (poly, twiddle)
    ...
    n − −
end while
add twiddle-ptr, #14             ▷ Incrementing twiddle-ptr by 14 for next stage
n ← 8
while n > 0 do                                   ▷ Second stage (Stage 4,5,6)
    m ← 2
    while m > 0 do
        load poly
        ldrh twiddle, [twiddle-ptr]              ▷ Loading twiddle from twiddle-ptr
        doublebutterfly (poly, twiddle)
        ldr twiddle, [twiddle-ptr, #2]           ▷ Loading twiddle from (twiddle-ptr+2)
        doublebutterfly (poly, twiddle)
        ...
        m − −
    end while
    add twiddle-ptr, #14         ▷ Incrementing twiddle-ptr by 14 for next stage
    n − −
    ...                                          ▷ Last stage (Stage 7)
end while
```

We utilize the optimized implementation of Kyber KEM from the *pqm4* library for 32-bit ARM Cortex-M4 based microcontrollers [KRSS19] for our analysis[2]. We compiled our implementations using the `arm-none-eabi-gcc` compiler, with the highest compiler optimization level `-O3`. We analyzed the compiled assembly code using an On-Chip Debugger to better understand the utilization of twiddle constants within the NTT/INTT computation.

Refer Alg.3 for a simplified pseudo-code of the assembly optimized NTT routine of Kyber. The twiddle constants are pre-computed and stored as a *constant* array at a

[2] Our analysis and experiments were carried out on the NTT implementations of Kyber and Dilithium corresponding to the commit hash `cf6f358c05db8a4e416561801bb4920d05b3bbb1`, and were available in the *pqm4* library until Jan 31, 2022. However, our attacks also apply in the same manner to the most recent NTT implementations in the *pqm4* library.

particular address in the flash memory (during compile time), denoted as T. This base address T of the twiddle constant array is also stored as a 32-bit value at a given location in the flash memory. Once the NTT routine is called, the base address T is first loaded from flash memory (in our case, the address is $(\mathsf{pc}+4)$ where pc is the program counter) into register $r1$ using the ldr instruction (Line 1 colored in red). The base address T in r1 is then used as a pointer to reference different constants in the twiddle constant array (Lines 8,10,15,21,23,28 colored in orange). We therefore refer to T as the twiddle pointer.

We make a key observation that the address for all the twiddle constants are calculated using the twiddle pointer T. If an attacker can fault the twiddle pointer from T to T^* (Line 1), then all the twiddle constants for the NTT are retrieved from a modified address T^*. If T^* points to a memory location filled with zeros, then all the twiddle constants are essentially zeroized with only a single fault. This, therefore serves as a *single point of failure* to zeroize all the twiddle constants of a target NTT, which we refer to as the twiddle-pointer vulnerability of the NTT. We also observe that the same vulnerability also exists in the optimized NTT implementations of Dilithium and Saber in the *pqm4* library. To zeroize the twiddle constants using a single fault, there are two main conditions:

1. Condition-1: Fault the twiddle pointer T to T^*, when loaded from flash memory.

2. Condition-2: The faulty twiddle pointer T^* points to an array filled with zeros.

3.2.1 Condition-1: Faulting Data Loaded from Flash Memory

Faulting the data loaded from flash memory to the register was first reported by Menu et al. [MBD+19] using Electromagnetic Fault Injection (EMFI) on an ARM Cortex-M3 based microcontroller. They demonstrated the ability to perform both bit-set and bit-reset faults on the fetched data, at a byte-level precision with upto 100% repetability. The same fault model has also been used in a recent work by Soleimany *et al.* [SBH+22] on the ARM Cortex-M4 microcontroller, to demonstrate Persistant Fault Analysis on block ciphers using EMFI. As we show later in Sec.6, we were also able to achieve the same fault model on a similar ARM Cortex-M4 device with a very high repeatability (upto 100%).

3.2.2 Condition-2: Retrieving Zero Data from Memory Access

We also require that the memory accesses from the faulty twiddle pointer T^* results in fetch of a zero twiddle constant array. This naturally raises a question of *how many locations in the target's addressable memory result in fetch of a zero array.* We therefore performed an empirical memory analysis on our DUT, (i.e.) STM32F407VG microcontroller (ARM Cortex-M4), to estimate the probability of fetching a zero array from a random 32-bit address. For each memory access, there are three possible outcomes: (1) Zero array - Success (2) Non-zero array - Failure and (3) Hard Fault due to illegal memory access - Failure. In several instances, we also observe that the CPU can fetch zero data, even if the faulty address is not mapped to a physical memory such as Flash/SRAM. For $10k$ random memory accesses, we obtained a reasonably high success rate of $\approx 25\%$ to retrieve a zero twiddle constant array.

After identifying fault parameters that satisfy both the conditions with high repeatability, during an initial profiling, the attacker can achieve 100% attack success as shown later in Sec. 6. Our practical experiments yield a very high fault repeatability (upto 100%) to zeroize all the twiddle constants using a single fault in both Kyber and Dilithium.

Remark on targeting the NTT input: Our analysis of the NTT implementations in Kyber and Dilithium revealed that coefficients of the NTT input are also accessed using a single pointer variable (denoted as input pointer P). On first glance, it might appear that a single fault on the input pointer P can also zeroize the entire NTT input. However, this pointer is not susceptible to EMFI, atleast in the same manner as the twiddle pointer. Unlike the *constant* twiddle array, whose pointer/address is fetched from the flash memory, the NTT input is a *variable* whose address P is calculated on the fly using arithmetic instructions, and not fetched from flash memory. Thus, the input pointer P is not exposed to EMFI in the same way as the twiddle pointer T. Moreover, it is not clear how P can be faulted using EMFI or other attack vectors.

Even if the attacker can fault the input pointer, there are significant challenges. The input pointer P is dynamically computed several times within a single execution of the target procedure in Kyber/Dilithium. All these computations need to be faulted to ensure that the faulty value is used throughout the computation. This is difficult to achieve in practice, and even otherwise requires very precise knowledge about the implementation at the assembly level. Given these challenges, we argue that the NTT's twiddle pointer serves as a much more realistic target for fault injection attacks.

4 Practical Attacks on Kyber

In this section, we propose novel key recovery and message recovery attacks on Kyber exploiting the twiddle-pointer fault vulnerability. Our analysis utilizes the algorithm of CPA secure PKE of Kyber in Alg.1 for explanation.

4.1 Key Recovery Attack

Our key recovery attack targets the NTTs in the key generation procedure, to generate public keys whose secret keys have a very low entropy. We propose to fault the NTT operation on the secret $\mathbf{s} \in R_q^k$ (Line 7). Let the faulty NTT output be denoted as $\hat{\mathbf{s}}^*$. Since $\hat{\mathbf{s}}^*$ is utilized to generate the LWE instance (Line 9), the LWE instance is implicitly created using a low-entropy secret $\mathbf{s}^*$. If all the k NTTs of $\mathbf{s}$ are faulted, then only the first two coefficients of every polynomial of $\mathbf{s}^*$ are non-zero, while all the other coefficients are zeros. For Kyber768 with $k = 3$ and the span of the coefficients in $[-2, 2]$, the faulty secret key $\mathbf{s}^*$ can be recovered from the public key with a brute-force complexity of 5^6 (= 15,625). We can utilize the following approach to arrive at the exact value of $\mathbf{s}^*$. For each guess of $\mathbf{s}^*$, we can compute the difference $\mathbf{d} = \mathbf{t} - \mathbf{A} \cdot \mathbf{s}^*$. The difference $\mathbf{d}$ for the correct guess will have a short span equal to that of the error of the LWE instance (i.e.) $[-2, 2]$. Once the target NTTs are faulted, the secret key can be recovered with a 100% success rate. We henceforth refer to this as the Kyber-Key-Recovery attack.

Since the secret key of Kyber is stored in the NTT domain, the same faulty secret is also used in the decryption procedure. Thus, the injected fault in the key generation procedure also propagates to the decryption procedure. Moreover, the faulty secret $\mathbf{s}^*$ is also valid, since $\ell_\infty(\mathbf{s}^*)$ respects that of a valid secret of Kyber. Thus, key recovery is successful while also maintaining the correctness of the scheme. Since the faulty public key is a valid LWE instance, it is indistinguishable from random, making it difficult to detect our attack, simply from analyzing the public key.

4.2 Message Recovery Attack

Our message recovery attack targets the encryption procedure of Kyber KEM. The aim is to recover the message from a valid ciphertext corresponding to a key-exchange between two parties (Alice and Bob). We propose to target the NTT of $\mathbf{r}$ in the encryption procedure (Line 17), which ensures use of a low-entropy $\mathbf{r}^*$ to generate the ciphertext. Similar to our key recovery attack, the brute-force complexity to guess $\mathbf{r}^*$ for Kyber768 is 5^6. If the correct $\mathbf{r}$ can be recovered, the secret message m can be recovered from the

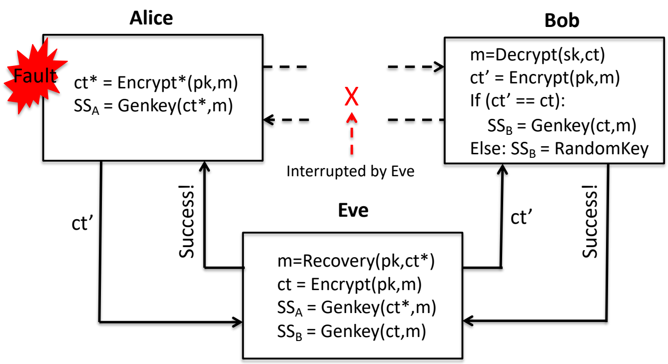

Figure 2: Fault assisted MITM attack on CCA Secure KEM scheme

faulty ciphertext ($ct^* = (\mathbf{u}^*, v^*)$) as follows:

$$m = \mathsf{Compress}(v^* - \mathsf{INTT}(\hat{\mathbf{t}} \circ \mathsf{NTT}(\mathbf{r})), 1)$$

Among the 5^6 possibilities for $\mathbf{r}^*$, the correct value of $\mathbf{r}^*$ can be recovered as follows. For a given guess of $\mathbf{r}^*$, the erronous message polynomial can be calculated as,

$$\mathbf{m} = \mathbf{v}^* - \mathsf{INTT}(\mathbf{t}^T \circ \mathbf{r}^*)$$

For the correct guess, the coefficients of $\mathbf{m}$ are clustered around 0 and $q/2$ with a short span, while for all other guesses, the coefficients are uniformly distributed in $\mathbb{Z}_q$. Once the target NTTs are faulted, the secret key can be recovered with a 100% success rate. We henceforth refer to this as the Kyber-Message-Recovery attack. The impact of our message recovery attack depends upon whether the attacker targets the (1) CPA Secure PKE or (2) CCA secure KEM of Kyber.

4.2.1 Attacking CPA secure Kyber PKE

The CPA secure PKE is typically used for ephemeral key exchanges. Faulting its encryption procedure results in creation of a faulty ciphertext. However, the faulty ephemeral secret $\mathbf{r}^*$ used to generate the ciphertext is valid, since $\ell_\infty(\mathbf{r}^*)$ respects that of a valid ephemeral secret. Since the decryption procedure does not check for the validity of the ciphertext, the correctness of key exchange is maintained, while also resulting in message recovery.

4.2.2 Attacking CCA secure Kyber KEM

The decapsulation procedure of CCA secure Kyber can detect the validity of a ciphertext with a very high probability. Thus, the faulty ciphertext is rejected by the decapsulation procedure. This is because the ephemeral secret $\mathbf{r}$ used in the encryption procedure (Alice) differs from that used in the re-encryption procedure after decryption (Bob). This leads to failure of the key exchange, thereby rendering message recovery useless. The attack only works if the attacker can fault the NTT of $\mathbf{r}$ in both the encapsulation and decapsulation procedure. However, this is a very strong assumption since the attacker requires access to both the communicating devices for a successful attack.

But, we observe that a Man-In-The-Middle (MITM) attacker can perform message recovery, while still ensuring the correctness of key-exchange between Alice and Bob. Refer to Fig.2 for a high-level illustration of the fault assisted MITM attack on CCA secure Kyber, with Eve as the MITM. The same setup was also utilized by Ravi *et al.* [RRB+19] for their message recovery attack on the encryption procedure. The function GenKey is used to derive a secret key from message m. The faulty encryption procedure is denoted as Encrypt*. The attack is carried out as follows: Eve faults the encapsulation procedure of Alice, resulting in a faulty ciphertext ct^* for message m and the corresponding shared key being $\mathsf{SS_A}$. Eve can recover m from the faulty ciphertext and thus compute the shared secret $\mathsf{SS_A}$ generated by Alice. Eve can now simply perform a valid key exchange with Bob whose shared secret key is $\mathsf{SS_B}$. With the knowledge of both $\mathsf{SS_A}$ and $\mathsf{SS_B}$, Eve can decrypt all communication between Alice and Bob.

4.2.3 Applicability to Saber:

We verified that the twiddle-pointer vulnerability is also present in the NTT implementations of Saber. Given the similarlity of Kyber and Saber, it is possible that our proposed key/message recovery attacks are also applicable to Saber in a straightforward manner. For brevity, we do omit our analysis of Saber in this paper.

5 Practical Attacks on Dilithium

In this section, we demonstrate two types of attacks on Dilithium exploiting the twiddle-pointer vulnerability: (1) Existential Forgery Attack and (2) Verification Bypass Attack. We utilize the algorithm of Dilithium in Alg.2 for our analysis.

5.1 Existential Forgery Attack

An attacker can forge signatures of Dilithum, if he/she is able to retrieve its primary secret $\mathbf{s_1}$. A close observation of the signing procedure reveals that the primary signature component $\mathbf{z}$ is closely dependent on s_1, and thus faulting the generation of $\mathbf{z}$ can reveal information about s_1. Generation of $\mathbf{z}$ (Line 24) is done as follows:

$$\begin{aligned}\mathbf{z} &= \mathsf{INTT}(\mathsf{NTT}(\mathbf{s_1}) \circ \mathsf{NTT}(c)) + \mathbf{y} \\ &= \mathsf{INTT}(\hat{\mathbf{s_1}} \circ \hat{c}) + \mathbf{y}\end{aligned} \tag{8}$$

Essentially, $\mathbf{z}$ is nothing but the ephemeral nonce $\mathbf{y}$, additively masked by the product $\mathbf{s_1} \cdot c$, where c is public and is part of the signature. For brevity, we refer to $\mathbf{s_1}$ as $\mathbf{s}$. For simplicity, our analysis assumes all operands in Eqn.8 are single polynomials in R_q. Since the polynomials in each operand are handled independently of each other, our analysis can be easily extended to all the polynomials in a straightforward manner. We present two novel key recovery attacks on both the deterministic and probabilistic/randomized variants of Dilithium. We assume that the attacker can trigger the target device to generate signatures for any message of his/her choice.

5.1.1 Attack-1: Targeting Deterministic Dilithium

Our first attack is a differential style fault attack targeting the signing procedure of deterministic Dilithium. Our target is the NTT of the challenge polynomial c. We recall that the challenge polynomial c is sparse with coefficients in $\{-1, 0, 1\}$, and the coefficients of c are represented as $(c_0, c_1, c_2, \ldots, c_{n-1})$. Our attack is carried out as follows: The attacker lets the target sign the message m, whose correct signature is $\sigma = (\mathbf{z}, \mathbf{h}, c)$. The message m is chosen such that the first coefficient of challenge c is 0 (i.e.) $c_0 = 0$. The attacker yet again lets the target sign m, but this time, the NTT of c is faulted to zeroize all its twiddle constants. As a result, the faulty $c^* = (c_0, 0, 0, \ldots, 0)$. Since $c_0 = 0$, the faulty challenge $c^* = 0$. As a result, the faulty signature $\mathbf{z}^*$ is given as:

$$\begin{aligned}\mathbf{z}^* &= \mathbf{s} \cdot c^* + \mathbf{y} \\ &= \mathbf{y} \quad (\because c^* = 0)\end{aligned} \tag{9}$$

which is nothing but the ephemeral nonce y. Thus, the difference between $\mathbf{z}$ and $\mathbf{z}^*$ ($\Delta\mathbf{z}$) simply yields the product $\mathbf{s}\cdot c$. Since c is known, $\mathbf{s}$ can be easily calculated as $\Delta\mathbf{z}\cdot c^{-1} \in R_q$.

The signing procedure follows the Fiat-Shamir with Aborts framework and thus presents additional challenges. Successful key recovery requires that both the valid and faulty signatures utilize the same number of iterations (κ) before exiting the abortion loop (i.e.) $\Delta(\kappa) = \kappa^* - \kappa = 0$. However, the use of faulty intermediate values do not always guarantee termination at the same iteration. Thus, not all successful faults result in key recovery.

We therefore performed empirical fault simulations using 1000 secret keys, assuming a perfect fault on the NTT of c. We observed that an average of ≈ 13 signatures are enough to recover the secret key with 100% success rate. We henceforth refer to this as the Deterministic-Dilithium-Forgery attack. Since the generated faulty signatures are invalid, verification after sign serves as an effective countermeasure against this attack.

5.1.2 Attack-2: Targeting Probabilistic Dilithium

The probabilistic signing procedure of Dilithium samples a random ephemeral nonce $\mathbf{y}$ for every execution (independent of the message m). This makes it impossible to know *apriori*, the number of iterations of the signing procedure for a given message m. Combined with the influence of non-constant time rejection checks, the operations in the signing procedure are *temporally randomized*, which makes it very difficult to perform injected targeted faults. Moreover, differential style fault attacks do not apply, since the computations are also randomized. Thus, mounting practical fault injection attacks on probabilistic Dilithium is very challenging, especially using targeted faults. We however show that the twiddle-pointer vulnerability can be exploited for key recovery over probabilistic Dilithium in certain settings.

The main target of our attack is the NTT over the ephemeral nonce $\mathbf{y}$ (Line 20). However, we observe that the current implementations of Dilithium calculate the primary signature $\mathbf{z}$ using $\mathbf{y}$ in the normal domain (Line 24). Thus, faulting the NTT of $\mathbf{y}$ does not reveal any information about $\mathbf{s_1}$. However, computing $\mathbf{z}$ in this manner is merely an implementation choice and it is possible that $\mathbf{z}$ can be alternatively computed as

$$\begin{aligned}\mathbf{z} &= \mathsf{INTT}(\mathsf{NTT}(\mathbf{s_1}) \circ \mathsf{NTT}(c) + \mathsf{NTT}(\mathbf{y})) \\ &= \mathsf{INTT}(\hat{\mathbf{s_1}} \circ \hat{c} + \hat{\mathbf{y}})\end{aligned} \tag{10}$$

Generating $\mathbf{z}$ in this manner also has an advantage of not requiring to retain/store $\mathbf{y}$ in memory, thereby reducing dynamic memory consumption by about 3.68 KB for Dilithium3. Thus, this alternative approach is attractive for a designer as a memory optimization. We however identify that this alternate approach makes it possible to perform key recovery in the following manner.

Firstly, operations in the probabilistic signing procedure are temporally randomized. We however observe that the NTT of $\mathbf{y}$ (Line 20) is performed before the first rejection check (Line 27). Thus, NTT of $\mathbf{y}$ in the first iteration, always occurs at a fixed time, from the start of the signing procedure, thereby making it possible to be targeted through fault injection. By faulting NTT of $\mathbf{y}$, $\mathbf{z}$ is computed using a low-entropy $\mathbf{y}^*$ and the faulty signature $\mathbf{z}^*$ is given as:

$$\mathbf{z}^*[i] = \begin{cases} \mathbf{sc}[i] + \mathbf{y}[i], & \text{for } i = 0 \\ \mathbf{sc}[i], & \text{for } 1 \le i < n-1 \end{cases} \tag{11}$$

where $\mathbf{sc}$ is the product $\mathbf{s}\cdot c$. Thus, all but the first coefficient of $\mathbf{sc}$ are exposed as part of the faulty signature $\mathbf{z}^*$. An attacker can simply guess the first coefficient of $\mathbf{sc}$ and subsequently calculate $\mathbf{s}$ for each guess, until he/she finds out the correct $\mathbf{s}$. The correct $\mathbf{s}$ can be found out by simply checking if the span of the recovered $\mathbf{s}$ (i.e.) $\ell_\infty(\mathbf{s})$ satisfies the bounds of a valid secret. A wrong guess will simply yield an $\mathbf{s}$ with a very large ℓ_∞ norm. For successful key recovery, the faulty signature and its associated intermediate variables should also satisfy all the rejection checks of the abortion loop.

We performed empirical fault simulations using 1000 secret keys and an average of ≈ 3 signatures are sufficient to recover the secret key with 100% success rate. To the best of our knowledge, we have presented the first practical fault injection attack applicable to the probabilistic variant of Dilithium, resulting in full key recovery without requiring any brute-force search. We henceforth refer to this attack as Probabilistic-Dilithium-Forgery. The faulty signature generated using the low entropy nonce $\mathbf{y}^*$ is valid and thus passes verification. Thus, the verification after sign countermeasure does not work against this attack, which makes it a more stealthier attack compared to the Deterministic-Dilithium-Forgery attack.

5.2 Verification Bypass Attack

While the aforementioned attacks target the signing procedure, the verification procedure also serves as a good target for fault injection attacks. One of the main motivation being, forceful acceptance of invalid signatures through faults, for any message of the attacker's choice. One of the obvious and known targets for fault injection is to simply skip the final comparison operation that decides the validity of the receieved signatures (Line 39). So, it is possible that the designer fortifies the comparison operation to protect against such trivial attacks. Bindel *et al.* [BBK] proposed a novel *zeroing fault* attack on the verification procedure of GLP and BLISS signature schemes. They show that zeroizing the challenge c during verification can force acceptance of invalid signatures. However, faulting an entire polynomial to zero is very difficult to achieve in practice. Moreover, the applicability of their attack to Dilithium is also not clear, considering the underlying differences between the signature schemes. In the following, we demonstrate exploitation of the twiddle-pointer fault vulnerability to present the first practical *zeroing fault* attack on the verification procedure of Dilithium.

For a given signature $\sigma = (\mathbf{z}, \mathbf{h}, c)$, the verification procedure computes $\mathbf{w_1}'$ (Line 37), which is further hashed with the message μ to recompute the challenge $\bar{c}$ (Line 38). Then, $\bar{c}$ is compared with the received challenge polynomial c, and the result of comparison determines validity of the signature. The main target of our attack is the NTT operation over c (Line 36). If $c_0 = 0$, then faulting NTT of c ensures that a faulty $\hat{c}^* = 0$ is used to compute a faulty $\mathbf{w_1}^*$, which is given as:

$$\begin{aligned} \mathbf{w_1}^* &= \mathsf{UseHint}(\mathbf{h}, \mathbf{A} \cdot \mathbf{z}) \\ c^* &= \mathcal{H}(\mu \| \mathbf{w_1}^*) \end{aligned} \tag{12}$$

We observe that faulty $\mathbf{w_1}^*$ is only dependent on $(\mathbf{h}, \mathbf{z})$, which an attacker is free to choose. We therefore propose to generate a malicious signature in the following manner:

Algorithm 4 Malicious Signing Procedure for Verification Bypass Attack

procedure MALICIOUS-SIGN(sk, M)
  $\hat{\mathbf{A}} \in R_q^{k \times \ell} \leftarrow \mathsf{Expand}(seed_A)$
  $\mu \in \{0,1\}^{512} \leftarrow \mathcal{H}(tr \| M)$
  while $c_0 = 0$ **do** ▷ Start of Abort Loop
    $\mathbf{z}^* \leftarrow \mathsf{Sample}_Z()$
    $\mathbf{h}^* \leftarrow \mathsf{Sample}_h()$
    $\mathbf{w}_1^* = \mathsf{UseHint}(\mathbf{h}^*, \mathbf{A} \cdot \mathbf{z}^*)$
    $c = \mathcal{H}(\mu, \mathbf{w}_1^*)$
  end while
  $\sigma = (\mathbf{z}, \mathbf{h}, c)$
end procedure

the attacker samples a random $(\mathbf{z}^*, \mathbf{h}^*)$ whose respective norms respect the conditions for successful verification. For a chosen message μ, he/she computes $\mathbf{w_1}^*$ and c^* as in Eqn.12, and repeats as until $c_0^* = 0$. Then, the attacker's crafted signature for μ is $\sigma^* = (\mathbf{z}^*, \mathbf{h}^*, c^*)$. Refer Alg.4 for an algorithmic description to create a malicious signature for our verification bypass attack.

In the attack phase, the attacker queries the verification procedure with (σ^*, μ) and faults the NTT over c^*. Since $c_0^* = 0$, the injected fault zeroizes the challenge c and thus computes the same $\mathbf{w_1}^*$ and challenge c^*, thereby resulting in successful verification. We performed empirical fault simulations using 1000 random messages and were able to enforce acceptance of invalid signatures for all the messages, thereby demonstrating a 100% success rate for our verification bypass attack. We henceforth refer to this as Dilithium-Verification-Bypass attack.

6 Experimental Validation

6.1 Experimental Setup

Our experiments are performed on the optimized implementations of Kyber and Dilithium, taken from the *pqm4* library, a benchmarking and testing framework for PQC schemes on the ARM Cortex-M4 family of microcontrollers [KRSS19]. Our DUT is the STM32F407VG microcontroller mounted on the STM32F4DISCOVERY board. The implementations are compiled using the `arm-none-eabi-gcc` compiler (with compilation options `-O3 -mthumb -mcpu=cortex-m4 -mfloat-abi=hard -mfpu=fpv4-sp-d16`) and run at a clock frequency of 168 MHz. The DUT contains cache lines for both instruction and data fetched from flash memory, to accelerate code execution and literal access. Both the instruction and data caches are therefore enabled to maximize performance. The communication with the DUT is done using UART.

We rely on Electromagnetic Fault Injection as our attack vector. Our EMFI setup comprises of three main components: (1) a high-voltage pulse generator capable of generating pulses up to 200V (in either polarity) with a very low rise time under 4ns; (2) a hand-crafted electromagnetic probe designed as a simple loop antenna; and (3) a motorised XYZ table to position the probe over the DUT. An optional oscilloscope is used for verification of pulse strength and timing characteristics. A software synchronizes the operation of the DUT and the EMFI setup, with faults injected based on a feedback signal from the DUT. Relay switches are also used for automated power-on reset of the DUT.

6.2 Performing Targeted Fault Injection

For our attack evaluation, we utilize a trigger signal from the DUT to signal the start of the target NTT to fault. However, an attacker can also utilize EM/power side-channel information to approximately narrow down the time window for fault injection.

6.2.1 Using Power/EM Analysis for Identification of Time Window

We utilize EM measurements acquired from the same DUT using a near-field EM probe, collected using a Lecroy 610Zi oscilloscope at a sampling rate of 500MSam/sec. The repetitive nature of operations in Module-LWE/LWR based schemes, as well as a preliminary knowledge of the implementation allows us to distinguish different operations. Refer Fig.3(a) for the EM trace from execution of the key generation procedure of Kyber768, where we annotate the trace with names of different operations. Refer Fig.3(b) for a zoomed-in-view of the trace which clearly shows the repeating patterns corresponding to the $k = 3$ NTTs of $\mathbf{s}$. We also confirmed through experiments that a similar technique

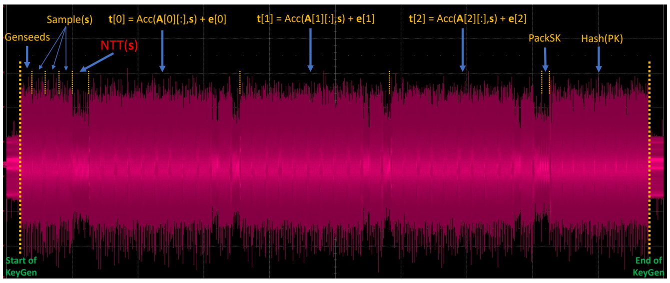

(a)

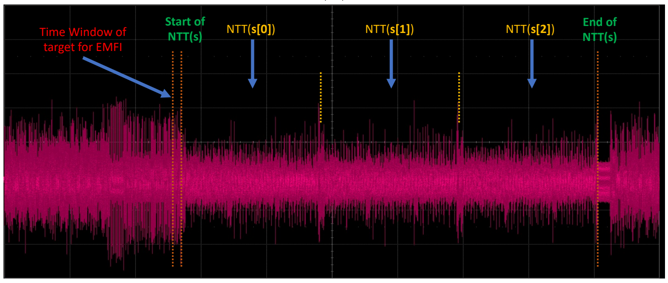

(b)

Figure 3: Visual Inspection of EM trace from key generation procedure of Kyber768 on the ARM Cortex-M4 microcontroller (a) Identification of repeating patterns and mapping to different operations (b) zoomed-in-view of trace corresponding to the $k = 3$ NTTs of $\mathbf{s}$

can be applied to the Kyber's encryption procedure as well as the signing and verification procedures of Dilithium (waveforms are omitted for brevity).

Upon roughly identifying the time window of the target NTTs, the attacker's main target is the twiddle-pointer loading operation that occurs just before the start of the NTT operation. Our EM side-channel analysis allows to narrow the time window to about 100-200 ns for fault injection.

6.2.2 Faulting Multiple NTTs in a Single Execution:

Our proposed attacks barring Deterministic-Dilithium-Forgery and Dilithium-Verification-Bypass, require to fault multiple NTT instances in a single execution. For instance, the Kyber-Key-Recovery attack requires to fault $k = 3$ NTTs of $\mathbf{s}$ in the key generation procedure, which would typically require 3 faults, one in each NTT. However, we observed through practical experiments that a single fault on the first NTT of a given module $\mathbf{s}$ (i.e.) $\mathbf{s}[0]$ propagates to the NTTs on all the other polynomials of $\mathbf{s}$ (i.e.) $\mathbf{s}[i]$ for $i \in [1, k-1]$. The same effect is also observed on Dilithium, when faulting $\mathbf{y} \in R_q^{\ell}$ with $\ell = 5$ NTTs. Moreover, the fault only propagates to the NTTs of the the same module, while not affecting the NTT over other modules.

We hypothesize that the aforementioned fault propagation behaviour could be due to reuse of the twiddle-pointer for NTTs of the same module. We recall that the data cache to the flash memory is enabled on our DUT. Hence, it is possible that the twiddle-pointer first retrieved from flash memory for NTT of $\mathbf{s}[0]$ is stored within the data cache, and the subsequent NTTs reuse the cached twiddle-pointer, without actually fetching from the flash memory. Thus, faulting the first fetch of the twiddle-pointer from flash memory ensures that a faulty value is also used for the subsequent NTTs of the same module. Thus, all our proposed attacks on both Kyber and Dilithium, require to inject only a single targeted fault in the target computation. This therefore serves as a best case scenario for an attacker, where a single fault is sufficient to fault multiple NTTs of the same module.

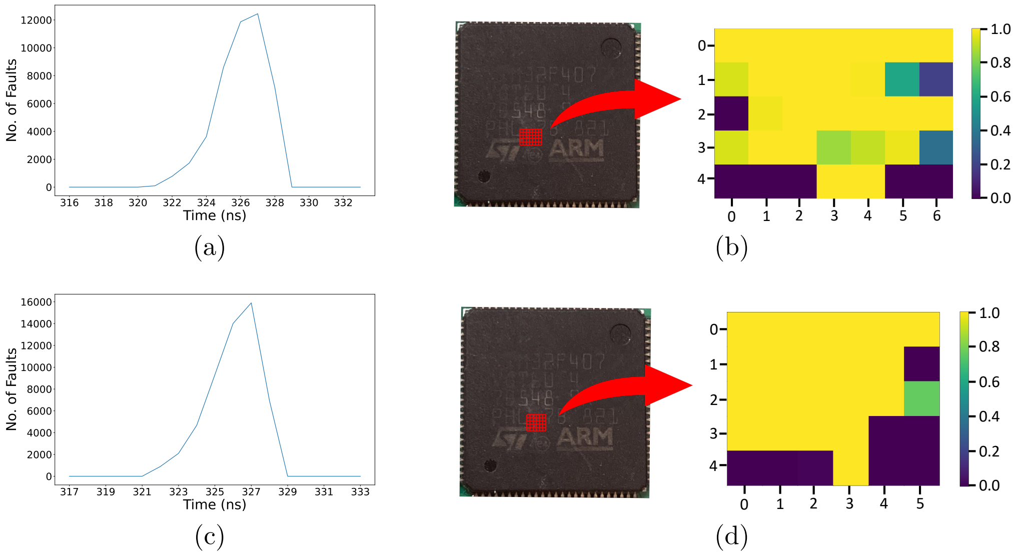

Figure 4: EMFI Results for Kyber-Key-Recovery (a,b) and Kyber-Message-Recovery (c,d) for Kyber768. (a,c) denotes sensitive time window, while (b,d) denotes best fault repetability achievable at different sensitive locations (XY) for the corresponding attacks.

6.3 Fault Injection Results

We consider the case of a profiled attacker who can profile the device and obtain the ideal set of fault injection parameters (i.e.) voltage (v), pulse-width (w), delay (d), x-y coordinate of the probe on chip (xy), that yields high repetability. We refer to a given set of values for the parameters (i.e.) (v_i, w_i, d_i, xy_i) as an *injection instance*. The number of repeated experiments performed at each injection instance is denoted as the *repetition* count.

To obtain injection instances that yield the best fault repeatability, we follow a two-step approach. We first perform a preliminary fault injection campaign, sweeping coarsely over a range of values for all the fault injection parameters, covering the entire area of the chip, and running 5 repetitions at each injection instance. Based on results from the preliminary campaign, we narrowed down the area for high fault repeatability, and run a more detailed campaign with 100 repetitions at each selected instance to calculate concrete numbers for fault repeatability. Results from the latter are presented in the following.

6.3.1 Kyber-Key-Recovery

We performed a total of 69300 fault injection experiments (i.e.) 100 experiments each at 693 favourable injection instances, to zeroize the twiddle constants of all the $k = 3$ NTTs of $\mathbf{s}$ in the key generation procedure of Kyber768. Among them, we obtained 46281 successful faults ($\approx 66\%$) and the number of successful faults against the injection delay is shown in Fig.4(a). We observe a narrow time window of about 7 ns in which we can observe a very high number of successful faults. Refer Fig.4(b) for the best fault repetability achievable (across voltage, pulse width and injection delay) as a function of the xy location of the injection probe on the chip's surface. We can observe that there are several fault injection instances (in a 1 mm $\times$ 1.5 mm area) that yield a high fault repetability upto 100%. We also tested our key recovery attack on 100 random faulty public keys obtained from one such fault injection instance. We were able to recover the secret key with 100% success rate, while the faulty public keys also resulted in correct key exchanges.

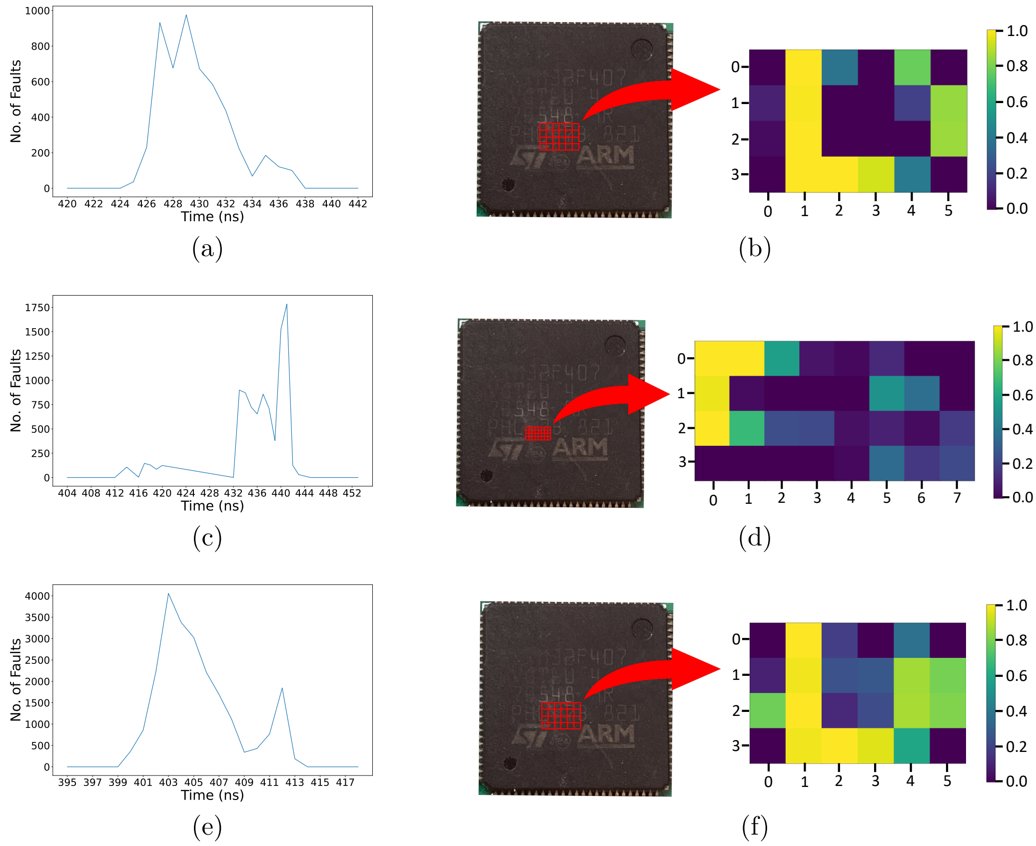

Figure 5: EMFI Results for Deterministic-Dilithium-Forgery (a,b) and Probabilistic-Dilithium-Forgery (c,d) and Dilithium-Verification-Bypass (e,f) for Dilithium3. (a,c,e) denotes Sensitive Time window, while (b,d,f) denotes best fault repetability achievable at different sensitive locations (XY) for the corresponding attacks.

6.3.2 Kyber-Message-Recovery

We performed 64600 fault injections to fault the $k = 3$ NTTs of the ephemeral secret $\mathbf{r}$ of Kyber's encryption procedure, among which we obtained 53844 successful faults ($\approx 83\%$). Refer Fig.4(c)-(d) for the corresponding fault injection results which very closely resembles the results of our Kyber-Key-Recovery attack. We yet again observe very high repetability of upto 100% at several fault injection instances. We also experimentally verified our message recovery attack on 100 random faulty ciphertexts, which yielded 100% success rate for recovering the message and the corresponding shared secret.

6.3.3 Deterministic-Dilithium-Forgery

We performed a total of 10100 fault injection experiments to fault the NTT of the challenge polynomial c in the signing procedure of deterministic Dilithium. We obtained a total of 5234 successful faults ($\approx 51\%$), all observed within a narrow time window of 13 ns (Refer Fig.5(a)). Refer Fig.5(b) for the cartography of the best achievable fault repetability (in a 1.5 mm $\times$ 2.5 mm area) on the DUT. This clearly shows several locations that yield high fault repetability upto 100%. We tested our attack on about 100 random faulty signatures and obtained a 100% success rate for key recovery.

6.3.4 Probabilistic-Dilithium-Forgery

We performed a total of 50300 fault injection experiments to fault all the $\ell = 5$ NTTs of the ephemeral nonce $\mathbf{y}$ in the signing procedure of probababilistic Dilithium. We obtained a total of 9155 successful faults ($\approx 26\%$), all observed within a slightly wider time window of 30 ns (Refer Fig.5(c)). Refer Fig.5(d) for the cartography of the best achievable fault repetability (in a 0.75 mm $\times$ 2 mm area), which again shows multiple locations that yield high fault repetability upto 100%. We tested our attack on about 100 random faulty signatures and obtained a 100% success rate for key recovery, while all the faulty signatures successfully passed the verification procedure.

6.3.5 Dilithium-Verification-Bypass

We performed a total of 35000 fault injection experiments the NTT of the challenge polynomial c in the verification procedure. We obtained a total of 22487 successful faults ($\approx 64\%$), all observed within a time window of 23 ns (Refer Fig.5(e)). Refer Fig.5(f) for the best fault repetability achievable as a function of the location injection probe on the chip's surface (in a 1.5 mm $\times$ 2.5 mm area), which again shows several locations that yield high fault repetability upto 100%. We also experimentally verified that invalid signatures for attacker's chosen messages were successfully verified with a 100% success rate.

6.3.6 Summary of Results

Thus, for all our targets, we observed between 26%-83% faults, that were successful when performing a detailed fault injection campaign for selected fault injection instances. The existence of yellow spots in Fig.4,5 clearly demonstrates the possibility to achieve high fault repeatibility for all of our presented attacks. Once an adversary has identified one such fault injection instance, the attack success rate is 100%.

7 Conclusion and Mitigation

In this paper, we have shown critical vulnerability in the implementation of NTT on *pqm4* library. Exploiting this vulnerability, termed as twiddle-pointer, we present practical and efficient attacks on Kyber and Dilithium. Few implementation-level countermeasures to eliminate the twiddle-pointer vulnerability can be considered.

On-the-fly Computation of Twiddle Factors: Instead of pre-computing the twiddle constants, one can adopt an on-the-fly approach to compute the twiddle constants for NTT/INTT, thereby eliminating the twiddle-pointer vulnerability. However, on-the-fly computation of the twiddle constants could impose a heavy performance penalty on the NTT/INTT.

Using Multiple Pointers for Twiddle Constants: Instead of relying on a single pointer to access the twiddle constants, one can utilize multiple twiddle pointers within the NTT, by splitting the array into multiple smaller arrays. While this increases the attacker's effort, it does not completely eliminate the vulnerability.

Utilization of Twiddle Constant Array in SRAM: Instead of using the twiddle constant array in the flash memory, one can simply copy the twiddle constants from flash into SRAM upon bootup/reset. Subsequently, all NTT/INTT computations utilize the twiddle constants in the RAM. However, this still leaves opportunity for potential persistent fault attacks.

Checking Entropy of NTT Output: The output of a valid NTT is typically uniformly random, while the output of our faulty NTT is heavily biased. Thus, checks on the distribution of the NTT outputs could help detect faults injected on the NTT computation.

Finally, while we demonstrate our attacks only on Kyber and Dilithium, we believe our analysis can be extended to other schemes such as Saber, NTRU and NTRU Prime, which also utilize NTT for polynomial multiplication. Our work stresses the need for concrete countermeasures against fault injection attacks for practical implementations of NTT, especially in embedded devices.

References

[AASA+20] Gorjan Alagic, Jacob Alperin-Sheriff, Daniel Apon, David Cooper, Quynh Dang, John Kelsey, Yi-Kai Liu, Carl Miller, Dustin Moody, Rene Peralta, et al. Status report on the second round of the NIST post-quantum cryptography standardization process. *US Department of Commerce, NIST*, 2020.

[ABD+20] Roberto Avanzi, Joppe W. Bos, Leo Ducas, Eike Kiltz, Tancrede Lepoint, Vadim Lyubashevsky, John Schanck, Peter Schwabe, Gregor Seiler, and Damien Stehlé. CRYSTALS-Kyber (version 3.0): Algorithm specifications and supporting documentation (October 1, 2020). *Submission to the NIST post-quantum project*, 2020.

[ACC+21] Erdem Alkim, Dean Yun-Li Cheng, Chi-Ming Marvin Chung, Hülya Evkan, Leo Wei-Lun Huang, Vincent Hwang, Ching-Lin Trista Li, Ruben Niederhagen, Cheng-Jhih Shih, Julian Wälde, et al. Polynomial multiplication in ntru prime: Comparison of optimization strategies on cortex-m4. *IACR Transactions on Cryptographic Hardware and Embedded Systems*, pages 217–238, 2021.

[ACC+22] Amin Abdulrahman, Jiun-Peng Chen, Yu-Jia Chen, Vincent Hwang, Matthias J Kannwischer, and Bo-Yin Yang. Multi-moduli ntts for saber on cortex-m3 and cortex-m4. *IACR Transactions on Cryptographic Hardware and Embedded Systems*, pages 127–151, 2022.

[AH21] Daniel Apon and James Howe. Attacks on NIST PQC 3rd Round Candidates, 2021. Invited talk at Real World Crypto 2021, `https://iacr.org/submit/files/slides/2021/rwc/rwc2021/22/slides.pdf`.

[BBK] Nina Bindel, Johannes Buchmann, and Juliane Krämer. Lattice-based signature schemes and their sensitivity to fault attacks. In *Fault Diagnosis and Tolerance in Cryptography (FDTC), 2016 Workshop on*, pages 63–77. IEEE.

[BKS19] Leon Botros, Matthias J Kannwischer, and Peter Schwabe. Memory-efficient high-speed implementation of kyber on cortex-m4. In *International Conference on Cryptology in Africa*, pages 209–228. Springer, 2019.

[BP18] Leon Groot Bruinderink and Peter Pessl. Differential Fault Attacks on Deterministic Lattice Signatures. *IACR Transactions on Cryptographic Hardware and Embedded Systems*, 2018(3), 2018. `https://eprint.iacr.org/2018/355.pdf`.

[CDH+19] Cong Chen, Oussama Danba, Jeffrey Hoffstein, Andreas Hülsing, Joost Rijneveld, John M Schanck, Peter Schwabe, William Whyte, and Zhenfei Zhang. NTRU: Algorithm specifications and supporting documentation (March 20, 2019). *Submission to the NIST post-quantum project*, 2019.

[CHK+21] Chi-Ming Marvin Chung, Vincent Hwang, Matthias J Kannwischer, Gregor Seiler, Cheng-Jhih Shih, and Bo-Yin Yang. Ntt multiplication for ntt-unfriendly rings: New speed records for saber and ntru on cortex-m4 and avx2. *IACR Transactions on Cryptographic Hardware and Embedded Systems*, pages 159–188, 2021.

[Coo66] SA Cook. On the minimum computation time for multiplication. *Doctoral diss., Harvard U., Cambridge, Mass*, 1, 1966.

[CT65] James Cooley and John Tukey. An Algorithm for the Machine Calculation of Complex Fourier Series. *Mathematics of Computation*, 19(90):297–301, 1965.

[DDLL13] Léo Ducas, Alain Durmus, Tancrède Lepoint, and Vadim Lyubashevsky. Lattice signatures and bimodal gaussians. In *Advances in Cryptology–CRYPTO 2013*, pages 40–56. Springer, 2013.

[DDP21] Jeroen Delvaux and Santos Merino Del Pozo. Roulette: Breaking kyber with diverse fault injection setups. *Cryptology ePrint Archive*, 2021.

[DKSRV20] Jan-Pieter D'Anvers, Angshuman Karmakar, Sujoy Sinha Roy, and Frederik Vercauteren. SABER: Mod-LWR based KEM (Round 3 Submission). *Submission to the NIST post-quantum project*, 2020.

[EFGT16] Thomas Espitau, Pierre-Alain Fouque, Benoît Gérard, and Mehdi Tibouchi. Loop abort faults on lattice-based fiat-shamir & hash'n sign signatures. *IACR ePrint Archive*, page 449, 2016.

[EFGT17] Thomas Espitau, Pierre-Alain Fouque, Benoît Gérard, and Mehdi Tibouchi. Side-Channel Attacks on BLISS Lattice-Based Signatures: Exploiting Branch Tracing Against strongSwan and Electromagnetic Emanations in Microcontrollers. In *Proceedings of the 2017 ACM SIGSAC Conference on Computer and Communications Security*, 2017.

[FO99] Eiichiro Fujisaki and Tatsuaki Okamoto. Secure integration of asymmetric and symmetric encryption schemes. In *Annual International Cryptology Conference*, pages 537–554. Springer, 1999.

[GLP12] Tim Güneysu, Vadim Lyubashevsky, and Thomas Pöppelmann. Practical lattice-based cryptography: A signature scheme for embedded systems. In *International Workshop on Cryptographic Hardware and Embedded Systems*, pages 530–547. Springer, 2012.

[GS66] W. Morven Gentleman and G. Sande. Fast fourier transforms: for fun and profit. In *American Federation of Information Processing Societies: Proceedings of the AFIPS '66 Fall Joint Computer Conference, November 7-10, 1966, San Francisco, California, USA*, volume 29 of *AFIPS Conference Proceedings*, pages 563–578. AFIPS / ACM / Spartan Books, Washington D.C., 1966.

[HPP21] Julius Hermelink, Peter Pessl, and Thomas Pöppelmann. Fault-enabled chosen-ciphertext attacks on kyber. In Avishek Adhikari, Ralf Küsters, and Bart Preneel, editors, *Progress in Cryptology - INDOCRYPT 2021 - 22nd International Conference on Cryptology in India, Jaipur, India, December 12-15, 2021, Proceedings*, volume 13143 of *Lecture Notes in Computer Science*, pages 311–334. Springer, 2021.

[IMS+22] Saad Islam, Koksal Mus, Richa Singh, Patrick Schaumont, and Berk Sunar. Signature correction attack on dilithium signature scheme. *arXiv preprint arXiv:2203.00637*, 2022.

[Kar63] Anatolii Karatsuba. Multiplication of multidigit numbers on automata. In *Sov. Phys. Dokl.*, volume 7, pages 595–596, 1963.

[KRSS19] Matthias J Kannwischer, Joost Rijneveld, Peter Schwabe, and Ko Stoffelen. pqm4: Testing and benchmarking NIST PQC on ARM Cortex-M4. In *Second PQC Standardization Conference: University of California, Santa Barbara and co-located with Crypto 2019*, pages 1–22, 2019.

[LDK+17] Vadim Lyubashevsky, Léo Ducas, Eike Kiltz, Tancrède Lepoint, Peter Schwabe, Gregor Seiler, Damien Stehlé, and Shi Bai. Crystals-dilithium. *Submission to the NIST Post-Quantum Cryptography Standardization [NIST]*, 2017.

[Lyu09] Vadim Lyubashevsky. Fiat-shamir with aborts: Applications to lattice and factoring-based signatures. In *International Conference on the Theory and Application of Cryptology and Information Security*, pages 598–616. Springer, 2009.

[MBD+19] Alexandre Menu, Shivam Bhasin, Jean-Max Dutertre, Jean-Baptiste Rigaud, and Jean-Luc Danger. Precise spatio-temporal electromagnetic fault injections on data transfers. In *2019 Workshop on Fault Diagnosis and Tolerance in Cryptography (FDTC)*, pages 1–8. IEEE, 2019.

[POG15] Thomas Pöppelmann, Tobias Oder, and Tim Güneysu. High-Performance Ideal Lattice-Based Cryptography on 8-Bit ATxmega Microcontrollers. In *Progress in Cryptology - LATINCRYPT 2015 - 4th International Conference on Cryptology and Information Security in Latin America, Guadalajara, Mexico, August 23-26, 2015, Proceedings*, pages 346–365, 2015.

[PP19] Peter Pessl and Robert Primas. More practical single-trace attacks on the number theoretic transform. In *International Conference on Cryptology and Information Security in Latin America*, pages 130–149. Springer, 2019.

[PP21] Peter Pessl and Lukas Prokop. Fault attacks on cca-secure lattice kems. *IACR Transactions on Cryptographic Hardware and Embedded Systems*, pages 37–60, 2021.

[PPM17] Robert Primas, Peter Pessl, and Stefan Mangard. Single-trace side-channel attacks on masked lattice-based encryption. In *International Conference on Cryptographic Hardware and Embedded Systems*, pages 513–533. Springer, 2017.

[RJH+19] Prasanna Ravi, Mahabir Prasad Jhanwar, James Howe, Anupam Chattopadhyay, and Shivam Bhasin. Exploiting determinism in lattice-based signatures: practical fault attacks on pqm4 implementations of nist candidates. In *Proceedings of the 2019 ACM Asia Conference on Computer and Communications Security*, pages 427–440, 2019.

[RPBC20] Prasanna Ravi, Romain Poussier, Shivam Bhasin, and Anupam Chattopadhyay. On configurable sca countermeasures against single trace attacks for the ntt. In *International Conference on Security, Privacy, and Applied Cryptography Engineering*, pages 123–146. Springer, 2020.

[RR21] Prasanna Ravi and Sujoy Sinha Roy. Side-channel analysis of lattice-based pqc candidates. *Round 3 Seminars, NIST Post Quantum Cryptography*, 2021.

[RRB+19] Prasanna Ravi, Debapriya Basu Roy, Shivam Bhasin, Anupam Chattopadhyay, and Debdeep Mukhopadhyay. Number "not used" once-practical fault attack on pqm4 implementations of nist candidates. In *International Workshop on Constructive Side-Channel Analysis and Secure Design*, pages 232–250. Springer, 2019.

[RVM+14] Sujoy Sinha Roy, Frederik Vercauteren, Nele Mentens, Donald Donglong Chen, and Ingrid Verbauwhede. Compact ring-LWE cryptoprocessor. In *International Workshop on Cryptographic Hardware and Embedded Systems*, pages 371–391. Springer, 2014.

[SBH+22] Hadi Soleimany, Nasour Bagheri, Hosein Hadipour, Prasanna Ravi, Shivam Bhasin, and Sara Mansouri. Practical multiple persistent faults analysis. *IACR Transactions on Cryptographic Hardware and Embedded Systems*, pages 367–390, 2022.

[Too63] Andrei L Toom. The complexity of a scheme of functional elements realizing the multiplication of integers. In *Soviet Mathematics Doklady*, volume 3, pages 714–716, 1963.

[XIU+21] Keita Xagawa, Akira Ito, Rei Ueno, Junko Takahashi, and Naofumi Homma. Fault-injection attacks against nist's post-quantum cryptography round 3 kem candidates. In *International Conference on the Theory and Application of Cryptology and Information Security*, pages 33–61. Springer, 2021.